



## Enhancing the inhibition potential of sodium tungstate towards mitigating the corrosive effect of *Acidithiobacillus thiooxidans* on X-52 carbon steel

Samuel E. Sanni<sup>a,\*</sup>, Ayomipo P. Ewetade<sup>a</sup>, Moses E. Emetere<sup>b</sup>, Oluranti Agboola<sup>a</sup>, Emeka Okoro<sup>c</sup>, Shade J. Olorunshola<sup>d</sup>, Taiwo S. Olugbenga<sup>d</sup>

<sup>a</sup> Department of Chemical Engineering, Covenant University, P.M.B 1023, Ota, Ogun State, Nigeria

<sup>b</sup> Department of Physics, Covenant University, P.M.B 1023, Ota, Ogun State, Nigeria

<sup>c</sup> Department of Petroleum Engineering, Covenant University, P.M.B 1023, Ota, Ogun State, Nigeria

<sup>d</sup> Department of Biological Sciences, Covenant University, P.M.B 1023, Ota, Ogun State, Nigeria

### ARTICLE INFO

#### Keywords:

Chemical inhibition  
Combined inhibitors  
Inhibitor efficiency  
Inhibition potential  
Microbial corrosion  
Optimum inhibitor concentration

### ABSTRACT

Microbial corrosion of the external surface of carbon steel pipes was investigated using sodium tungstate, sodium nitrite and zinc nitrite as individual and combined inhibitors. The study involved carbon steel pipes in contact with *Acidithiobacillus thiooxidans*. Inhibitor efficiencies were determined and the optimum inhibitor concentration required to effectively limit the corrosive effect of the microbe was 51–52 g/L for the best inhibitor. Also, despite the limiting effect of sodium nitrite in its other inhibitor formulations, its presence in the mixture of all three components, improved the performance of the other two chemicals giving the best inhibition efficiency of 85.68%.

### 1. Introduction

Corrosion of pipelines by microbes is prevalent in pipes carrying fluids which lie on the earth surface. In some cases, the pipes are buried in the ground or in contact with ground water which serves as a carrier of microbes that aid pipe corrosion. Microbial corrosion can be controlled via chemical inhibition. One very good chemical for impeding this form of corrosion on carbon steel is sodium tungstate. Several prior studies have revealed the corrosive nature of some microbes in soils where underground pipes are situated. Al-Jaroudi et al. [1] studied the failure of a 28-inch diameter, 25.5 km long underground pipeline transporting wet sour Arab-light crude caused by microbial corrosion. The ultrasound testing results showed localized pitting at failed locations while experimental investigations revealed that the failure was as a result of microbial corrosion favoured by low flow velocities, high water-cut and the presence of sulfur in the crude. Aruliah et al. [2] gave a study on the biodegradation of corrosion inhibitors by *Bacillus Cereus* and their influence on a pipeline conveying diesel using the rotating cage method. Cantero-Valencia and Periá-Carriales [3] discussed the corrosive effects of thermophilic Sulfate-Reducing Consortia on carbon steel, while the effect of nitrate on the morphology and activity of bacterial biofilm communities in pipelines used for seawater injection

into oil fields was studied by Carsten et al. [4]. New views on corrosion of iron by sulfate reducing bacteria were presented by Dennis and Julia [5] where they mentioned a few additional mechanisms for corrosion of iron by sulfate reducing bacteria. Hector et al. [6] carried out an extensive review on bio-corrosion and biofouling of industrial equipment where real time monitoring concepts of environmentally friendly approaches for understanding and mitigating metal decay were itemized. Accelerated cathodic reaction of a metal stimulated by the uptake of electrons by Sulfate Reducing Bacteria was studied by Hendrick et al. [7], in which they asserted that, an inhibitor may be added to the surface of the metal or alloy in order to decrease or mitigate its corrosion rate/microbial corrosion tendency [8]. According to Iversen [9], an example of microbe-aided/microbiologically induced corrosion (MIC) is one caused by the production of sulfuric acid by the action of *Thiobacillus* in some buried steel pipes. Lin and Ballim [10] investigated current approaches on biocorrosion control and their promising alternatives while Wu et al. [11] is a study that investigates the synergistic effect of superficial stress and sulfate reducing bacteria in relation to promoting hydrogen permeation through X80 steel pipeline, where it was observed that, the microbes in the soil where the pipe was located, as well as the surface stress induced on the metal, enhanced further permeation of hydrogen gas through the metal thus promoting/

\* Corresponding author.

E-mail addresses: [adexz3000@yahoo.com](mailto:adexz3000@yahoo.com) (S.E. Sanni), [ayomipo69@gmail.com](mailto:ayomipo69@gmail.com) (A.P. Ewetade), [moses.emetere@covenantuniversity.edu.ng](mailto:moses.emetere@covenantuniversity.edu.ng) (M.E. Emetere), [oluranti.agboola@covenantuniversity.edu.ng](mailto:oluranti.agboola@covenantuniversity.edu.ng) (O. Agboola), [emeka.okoro@covenantuniversity.edu.ng](mailto:emeka.okoro@covenantuniversity.edu.ng) (E. Okoro), [shade.olorunshola@covenantuniversity.edu.ng](mailto:shade.olorunshola@covenantuniversity.edu.ng) (S.J. Olorunshola), [taiwo.olugbenga@covenantuniversity.edu.ng](mailto:taiwo.olugbenga@covenantuniversity.edu.ng) (T.S. Olugbenga).

<https://doi.org/10.1016/j.mtcomm.2018.12.010>

Received 7 June 2018; Received in revised form 9 November 2018; Accepted 13 December 2018

Available online 02 February 2019

2352-4928/ © 2019 Elsevier Ltd. All rights reserved.

speeding up cathodic corrosion. In a similar study, despite the independent nature of applied stress and physiological activity of the bacterial strain, it was recorded that SRB and induced stress on same steel type, can synergistically induce mechano-chemical effects on the metal surface [12]. Batmanghelich et al. [13] investigated the corrosion tendencies of cast iron in the presence of *Pseudomonas Aeruginosa* (a denitrifying bacteria) and *Desulfovibrio Vulgaris* (DV- a sulfate reducing bacteria) where they observed that, cast iron corrosion diminished in the presence of both microbes relative to when it was in contact with the SRB only, whereas, the work of Jia et al. [14] holds the view that electron transfer mediators such as riboflavin and flavin adenine dinucleotide can help to accelerate the corrosive influence of *Pseudomonas Aeruginosa* on carbon steel. Liu et al. [15] also observed that, 7-day old extracellular polymeric extracts of an iron oxidizing bacteria helped to inhibit microbial corrosion at an optimum concentration of 240 mg/l whereas, higher or lower concentrations did not. Muthukumar et al. [16] carried out a review on microbiologically influenced corrosion of pipelines carrying petroleum products and based on the reports, it is necessary to identify the nature of the microbial population in a place in order to identify the suitable approach required for controlling their corrosive effects on the pipelines. Ngobiri et al. [17] carried out a comparative study on inhibitor performance for *Sulfadoxine–Pyrimethamine* (SP) and an industrial inhibitor during the corrosion of a petroleum steel pipe. Their findings revealed that SP has higher inhibitive power relative to the industrial inhibitor. Jia et al. [18] carried out a study that revealed the effect of biogenic H<sub>2</sub>S in an ATCC culture of *Desulfovibrio Vulgaris* and found that, the H<sub>2</sub>S released from its microbial activity accelerated corrosion of the carbon steel due to the increased sessile cell count thus causing a resultant thinning of the iron oxide film formed; a similar investigation was carried out using 2205 Duplex stainless steel [19] and 2304 stainless steel [20], while the work of Li et al. [21] revealed the potency of D-phenylalanine in the inhibition of Q235 carbon steel. Microbial corrosion in petroleum pipelines is a major problem in oil and gas fields as many oil companies in the world today, spend a major part of their revenue in the fight against corrosion [22]. The resulting effect may be seen as surface or internal damage of these pipelines. According to Vonwolzogen et al. [23], sulfate reducing bacteria has the ability to oxidize molecular hydrogen generated at cathodic sites which in turn facilitates cathodic depolarization hence resulting in corrosion. Pipe microbial corrosion refers to the destructive action of microbes on metallic pipes resulting from the reaction between the environment, fluid and micro-organisms. Amongst the established methods of control, is the chemical inhibition method which involves the use of chemical compounds as control mechanisms for microbial and other forms of corrosion. One of such inhibitors is sodium tungstate. It is an intermediate product of the conversion of tungsten ore to its metal [24]. Bioreactor simulation of a reservoir situation for the control of biosulfide production was carried out by Xue and Voordouw [25] using glutaraldehyde and benzalkonium chloride, with cocodiamine as biocides and nitrate source respectively. This paper focuses on the inhibition of the corrosive action of *Acidithiobacillus thiooxidans* on the external surface of carbon steel pipes by chemical injection because according to literature, pipe microbial corrosion is more severe at the surface relative to its internals. *Acidithiobacillus thiooxidans* is predominantly present in moist soils and ground waters. It takes the microbe 3–5 days to corrode a carbon steel pipe and if such effect is spread over a month/one year, it is obvious that the damage would be severe. Sodium Tungstate, although expensive, is used as inhibitor because it is readily available, however, when combined with other inhibitors, the total cost incurred from its use becomes friendly.

Corrosion of pipelines by *Acidithiobacillus thiooxidans* is very common with surface, buried/submerged pipes especially in environments where their metabolic activities are not restricted. However, since the microbe's activity can be impeded by sodium tungstate, this research then seeks to uncover a mixed inhibitor that has never been

reported in literature for improved performance of sodium tungstate.

## 2. Method

### 2.1. Equipment, materials and reagents

The materials used for this research are as follows: metal steel pipes, *Thiobacillus* agar, *Thiobacillus* broth, ground water sample from Onikolobo Abeokuta in Ogun state in Nigeria, syringe (5 ml), an Incubator (Vision Scientific, LIB-211-E, 220 V, 600 W), a refrigerator (Haier Thermocool, HDR-211-SX, 220–240 V/50 Hz, 110 W), ethanol (SIGMA-ALDRICH Ethanol Absolute), Emery paper (sand paper), sodium tungstate (Fischer Scientific, UK), zinc nitrite powder (Lab Tech Chemicals), water, measuring cylinder, beakers, brush, stop watch, hand gloves, weighing balance (Scout Pro, SPU 2001, 12 V AC), Shinadzu FTIR 8400S Spectrophotometer, Joel Field Emission Electron Microscope JESM-7600 F, Linear Polarization Resistance Meter PGSTAT101 made by Autolab, An Lb 1290 compound digital LCD inverted biological microscope with 5 MP wide field and infinite optical system

### 2.2. Procedure

#### 2.2.1. Preparation of the microbial culture (broth) and microbe isolation

The 5 ml syringe was used to suck some ground water which was used in making the *thiobacillus* broth (culture). The *thiobacillus* broth was placed in the incubator at a temperature of 28 °C and kept for 7 days to allow for microbial growth. Thereafter, isolation of the microbe that grew on the thiobacillus broth using *thiobacillus agar* was done, and was later subcultured in a liquid medium containing thiosulphate salts. The mixture was then stored in a refrigerator to keep the microbe alive but inactive.

#### 2.2.2. Preparation of carbon steel pipes for corrosion test

Ten (10) pipe samples made of carbon steel, of length 30 cm, each having a diameter of 2-inches, were cut off from a lengthy pipe. The samples were devoid of impurities by the use of emery paper. The samples were then washed with ethanol so as to prepare their surfaces after which the samples were dried.

#### 2.2.3. Preparation of sodium tungstate (inhibitor) solution

The measuring cylinder was used to transfer 1 L of water into a beaker. 50 g of sodium tungstate was measured on a weighing balance and poured into a beaker containing water. The contents of the beaker were thoroughly mixed to give sodium tungstate solution.

#### 2.2.4. Preparation of sodium tungstate and zinc nitrite (co-inhibitor) solution

With the measuring cylinder, 1 litre of water was transferred into a beaker. 50 g each of sodium tungstate and zinc nitrite were measured separately on a weighing balance and poured into a beaker containing 1 litre of water.

#### 2.2.5. Preparation of sodium tungstate with zinc nitrite and sodium nitrite as co-inhibitors in solution

Using a measuring cylinder, 1 litre of water was transferred into a beaker. 50 g each, of sodium tungstate, zinc nitrite Zn(NO<sub>2</sub>)<sub>2</sub> and sodium nitrite (NaNO<sub>2</sub>) were then added simultaneously and the resulting mixture was stirred thoroughly.

### 2.3. Corrosion tests

All tests were carried out at ambient condition i.e. at 30 °C.

### 2.3.1. Corrosion tests with inhibitor(s)

- (i) Pipe samples with one inhibitor only (i.e. sodium tungstate only, sodium nitrite only and zinc nitrite only)

Three carbon steel pipe samples of 30 cm length and 2-inches diameter labeled A, B, C were cleaned, dried and weighed on a weighing balance. The weights were recorded as  $w_{A1}$ ,  $w_{B1}$ ,  $w_{C1}$  respectively. Three separate solutions of 10 ml sodium tungstate, 10 ml sodium nitrite and 10 ml zinc nitrite solutions were drawn and dispersed over the pipe samples A, B and C respectively using a syringe. Three separate 15 ml portions of the corroding agent (*Acidithiobacillus thiooxidans*) were drawn and dispersed over each of the pipe samples. After 48 h, the pipes were cleaned to remove the corrosion products. The pipes were then brushed and rinsed with ethanol after which they were dried and reweighed. Their new weights  $w_{A2}$ ,  $w_{B2}$  and  $w_{C2}$  were determined with their corrosion rates and inhibitor performances respectively. The process was continued for a period of 288 h and data was recorded at an interval of 48 h. This test was carried out thrice for each pipe sample in order to ensure accuracy and reproducibility.

- (ii) Pipe Sample with Sodium Tungstate and Sodium Nitrite as Co-inhibitor

A carbon steel pipe labeled D, of length 30 cm, 2-inches diameter was cleaned, dried and weighed with a weighing balance and the weight ( $w_{D1}$ ) was recorded. A mixture containing 10 ml each of sodium tungstate and sodium nitrite solution was drawn, shaken and dispersed on the pipe sample using a syringe. 15 ml of the corroding agent (*Acidithiobacillus thiooxidans*) which was dispersed over the carbon steel pipe using another syringe. After 48 h, the pipe was ridden off its corrosion product using a brush after which it was rinsed with ethanol. The pipe sample was dried and weighed with the weighing balance and the weight was recorded as  $w_{C2}$ . The respective weights, corrosion rate and inhibitor performance were then determined. The process was also continued for a total time of 288 h with data taken at 48-hour interval. This test was carried out thrice for the pipe sample in order to ensure accuracy and reproducibility.

- (iii) Pipe Sample with Sodium tungstate and Zinc Nitrite (Co-inhibitor)

The procedure for case (ii) was repeated for the pipe sample labeled E of 30 cm length and 2-in diameter. The initial weight of the pipe was recorded as  $w_{E1}$  before applying the corroding agent (*Acidithiobacillus thiooxidans*), thereafter, a mixture of 10 ml each of sodium tungstate and zinc nitrite was made, properly mixed and applied over the pipe surface. 15 ml of the corroding agent was also drawn and applied to the pipe surface. The final weight of the pipe ( $w_{E2}$ ), alongside the corrosion rate and inhibitor performance were determined and recorded. This test was carried out thrice for the pipe sample in order to ensure accuracy and reproducibility.

- (iv) Pipe Sample with Sodium Nitrite and Zinc Nitrite (Co-inhibitor)

The procedure for case (iii) was also repeated for a pipe sample labeled F, of 30 cm length and 2-in diameter, with the initial weight recorded as  $w_{F1}$  before applying the corroding agent and inhibitor; but here, a 20 ml mixture each containing 10 ml of sodium nitrite and zinc nitrite was drawn with a syringe, shaken and applied over the pipe surface with 15 ml of the corroding agent (*Acidithiobacillus thiooxidans*). The final weight of the pipe ( $w_{F2}$ ), alongside the corrosion rate and inhibitor performance were determined and recorded. This test was carried out thrice for the pipe sample in order to ensure accuracy and reproducibility.

- (v) Pipe Sample with Sodium Tungstate and Two Co-inhibitors (Zinc

### Nitrite and Sodium Nitrite)

A Carbon steel pipe sample labeled G, was cleaned, dried and weighed. The weight ( $w_{G1}$ ) was recorded. A 30 ml solution containing 10 ml, each of sodium tungstate, zinc nitrite and sodium nitrite was measured and dispersed on the sample using a syringe. Another syringe was used to draw up 15 ml of the corroding agent (*Acidithiobacillus thiooxidans*) which was then spread over the carbon steel pipe. After 48 h, the pipe was cleaned to remove the corrosion product after which it was brushed and rinsed with ethanol. The sample was then dried and reweighed. The weight ( $w_{G2}$ ), the corrosion rate and inhibitor performance were determined. The process was continued for a period of 288 h while taking data at 48 h interval. This test was carried out thrice for the pipe sample in order to ensure accuracy and reproducibility.

### 2.3.2. Corrosion tests without inhibitor(s)

Three clean and dry carbon steel pipe samples, with equal dimensions as other pipe samples labelled H (pipe in contact with *Acidithiobacillus thiooxidans* without any form of protection but subjected to aerobic condition) I (pipe in contact with *Acidithiobacillus thiooxidans* without any form of protection but subjected to anaerobic condition) and J (pipe not contacted with *Acidithiobacillus thiooxidans* and without any form of protection but subjected to aerobic condition) were weighed and their initial weights  $w_{H1}$ ,  $w_{I1}$  and  $w_{J1}$  were recorded respectively. Two syringes were used to take 15 ml of the microbe and dispersed on the first two pipe samples which were subjected to the conditions stated above. The third pipe sample was neither contacted with inhibitor nor *Acidithiobacillus thiooxidans* but subjected to aerobic condition. After 48 h, the pipes were cleaned, brushed and rinsed with ethanol before they were dried and reweighed. Their new weights ( $w_{H2}$ ,  $w_{I2}$  and  $w_{J2}$ ) and corrosion rates were then determined. The entire process was repeated through 288 h with data taken at an interval of 48 h. This test was carried out thrice for each pipe sample in order to ensure accuracy and reproducibility.

### 2.4. Determination of corrosion rate

There are several techniques for monitoring corrosion rates. Corrosion control involves managing or protecting a surface against corrosion. Here, emphasis are on weight loss and linear resistance methods. Weight loss method, involves measuring the loss in weight of the carbon steel pipes after being exposed to the corroding agent. The rate of corrosion of a material is proportional to the weight loss per time and is given by the expression below:

$$C_R \propto \frac{W'}{t}$$

where:

$W'$  = loss in weight of metal due to corrosion

$t$  = time interval

$C_R$  = corrosion rate

Then introducing a constant,  $1/A$  i.e. per cross-sectional area gives

$$C_R = \left( \frac{W_0 - W}{At} \right) = W'/At \quad (1)$$

where:

$W_0$  = weight of the sample before contact with the corroding agent

$W$  = weight of the sample after contact with corroding agent

$A$  = total surface area

$t$  = time interval of exposure/immersion

### 2.5. Estimation of inhibitor efficiency

The efficiency of an inhibitor is a measure of the drop or reduction in corrosion rates by the introduction of inhibitor in the corrosive medium before it is applied to the surface of the pipes.

$$\eta = \left( \frac{C_{R0} - C_{R1}}{C_{R0}} \right) * 100\% \tag{2}$$

where:

$C_{R0}$  and  $C_{R1}$  are the corrosion rates of the samples when in contact with no inhibitor or various concentrations of inhibitors respectively.

$\eta$  = inhibitor efficiency

Other parameters:

Weight of empty syringe = 4.2 g

Weight of syringe + microbe = 9.6 g

Weight of microbe = 9.6 g – 4.2 g = 5.4 g

Volume of microbe used = 5 ml

Density of microbe =  $5.4/5 \times 10^{-3} = 1080 \text{ g/l}$

$$\text{Area of pipe (cylinder)} = 2\pi rh + 2\pi r^2 \tag{3}$$

Diameter = 2 in.; Radius = 1 inch = 0.0254 m

Height (length) = 30 cm = 0.3 m

$$\text{Therefore, Area} = [2 \times 3.142 \times 0.0254 \times 0.3] + [2 \times 3.142 \times 0.0254^2]$$

A = 0.05193 m<sup>2</sup>

Time interval = 48 h

### 2.6. Determination of optimum inhibitor concentration

To get the optimum inhibitor concentration, single, two and three inhibitor combinations were made. Also a time interval of 24 h was chosen for each increase in concentration of the inhibitor. A preliminary run was done to see if any optimum for the pipe samples resides between 0 and 45 g/l inhibitor concentration, however, since no optimum was obtained, it was then chosen as the start-up concentration. Three clean pipe samples (K, L and M) were washed with ethanol and properly dried. Their initial weights were recorded. Using a syringe, 15 ml of the microbe was drawn with 20 ml (in the ratio 1:1) of the two inhibitor combinations of interest or 10 ml each of the three inhibitors with compositions in the ratio 1:1:1. Different inhibitor concentrations were then used at different times in order to obtain the point where there is no further loss in weight of the pipe samples.

### 2.7. Statistical investigation of the weight loss method

The average mean weights of the pipe samples were determined statistically. Also, the modified Gumbel equation given by (4) was applied. The modified Gumbel distribution equation is a popular tool used for corrosion analysis [26,27]. The modified Gumbel distribution is shown below

$$P(x) = \frac{\lambda(m(t_i) - m(t_{i-1}))^x}{x!} \exp[-\lambda(m(t_i) - m(t_{i-1}))] \tag{4}$$

$\lambda$  is defined as the mean density per unit area,  $m(t_i)$  is the initial weight,  $m(t_{i-1})$  is the immediate weight reduction, and  $x$  is the number of trials. The modified Borel distribution as discussed in Finner et al. [28] was also considered here.

### 2.8. Tafel polarization measurements

Using a similar approach as discussed in Kumari et al. [29], Tafel polarization data was obtained for the corrosion rate of the metal where the corrosion rate of the carbon steel was determined using (5) while the surface coverage was determined using (6).

$$CR \text{ (mmpy)} = (3270 * M * i_{corr}) / \rho * Z \tag{5}$$

$$\Theta = i_{corr} - i_{corr(inh)} / i_{corr} \tag{6}$$

Where:

$\Theta$  = surface coverage

$i_{corr}$ ,  $i_{corr(inh)}$  = corrosion current densities without inhibitor and in

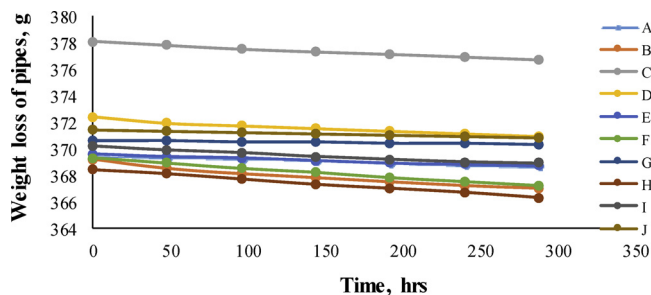


Fig. 1. Weight reduction of pipes A–J at different times.

the presence of inhibitor respectively [30].

### 3. Results and discussion

From Fig. 1, it can be seen that between 0 and 288 h, there is a slight reduction in weight for all pipe samples, when in contact with the microbe. It was 0.22% for pipe A when sodium tungstate was used as the only inhibitor, 0.6% for pipe B when sodium nitrite was used as the only inhibitor, 0.37% for pipe C when zinc nitrite was used as the only inhibitor, 0.4% for pipe D when sodium tungstate and sodium nitrite were used as combined inhibitor, 0.24% for pipe E when sodium tungstate and zinc nitrite were combined, 0.57% for pipe F when sodium nitrite and zinc nitrite were combined as inhibitors, 0.081% for pipe G when sodium tungstate, sodium nitrite and zinc nitrite were used as inhibitors, 0.57% for pipe H without any inhibitor and under aerobic condition, 0.35% for pipe I without any inhibitor and under anaerobic condition while it was 0.08% for pipe J. Based on the results, pipe B gave the highest corrosion rate.

Fig. 2 is an illustration of the corrosion rates of pipes A, B and C. The rate of corrosion of pipe A was found to be steady (constant) from 0 to 144 hrs. It increased by 100% over the previous value and remained steady between 192 h and 240 h respectively, and dropped by 50% at 288 h. The rate of corrosion of pipe B dropped by about 50% from 0 - 48 h and was 0.1605 g/m<sup>2</sup>hr after 96 h. It then dropped to 0.1204 g/m<sup>2</sup>hr in 144 h and remained steady at 0.0802 g/m<sup>2</sup>hr up to 240 h. Thereafter, it dropped to 0.0401 g/m<sup>2</sup>hr and remained steady throughout till 288 h.

Among all the three single inhibitors used, it could be seen that sodium tungstate posed the highest resistance to microbial corrosion. Zinc nitrite was second to it as shown in Fig. 2 while sodium nitrite showed the least inhibitive ability against the action of *Acidithiobacillus thiooxidans*.

Having calculated the differences in initial and final weights of Pipes D, E and F respectively, the graphical presentation in Fig. 3 shows the corrosion rates of the three pipe samples.

The corrosion rate of Pipe D rose from 0 to 0.2006 g/m<sup>2</sup>hr and remained so for 48 h. It then dropped to 0.0802 g/m<sup>2</sup>hr in the next hour

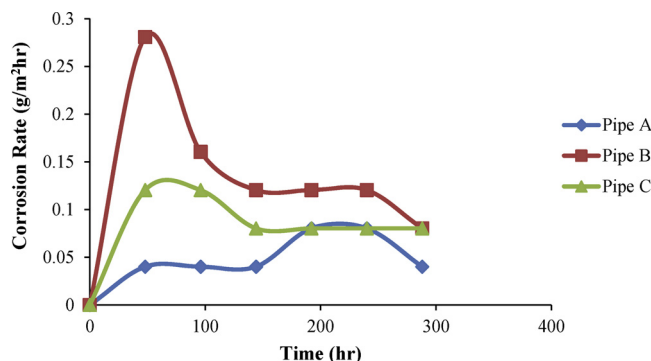


Fig. 2. Variation of corrosion rates of pipes A, B and C with time.

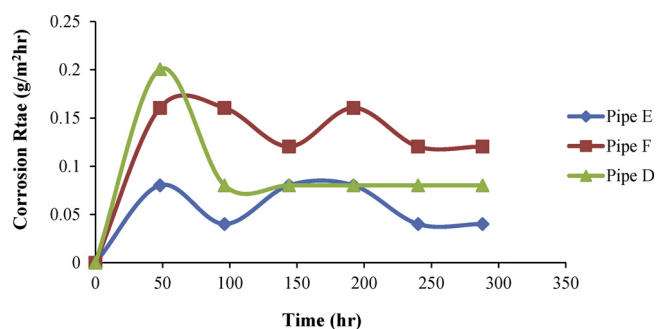


Fig. 3. Pipe corrosion rate vs time for pipes D, E & F.

and remained constant for the next 240 h. This simply implies that the effect of the inhibitor was significant after 48 h because of the drastic reduction (i.e. 60% reduction) in the corrosion rate of pipe D by the combined inhibitors (sodium tungstate and sodium nitrite). However, comparing the corrosion rates of pipes A and D as shown in Figs. 2 and 3 respectively, it is clear that sodium tungstate when used alone, is a better inhibitor than when combined with sodium nitrite because, for the former, pipe corrosion rate was maintained between 0.0401 and 0.0802  $\text{g/m}^2\text{hr}$  while for the latter, it was in the range of 0.0802 and 0.2006  $\text{g/m}^2\text{hr}$ . The higher corrosion rate recorded for pipe D is due to the unfavourable interaction of the sodium nitrite and sodium tungstate which resulted in lowering the total resistance posed by sodium tungstate thus reducing its inhibitive potential.

The hourly corrosion rate for Pipe E was 0.0802  $\text{g/m}^2\text{hr}$  for the first 48 h and later dropped by 50% for the next 48 h. There was a rise in hourly corrosion rate from the previous value between 144 and 192 h. It then dropped by 50% the following hour and was constant between 240 and 288 h; thus, comparing the results for pipes B and E as in Figs. 2 and 3 respectively, one could see the advantage of combining sodium tungstate and sodium nitrite over the use of sodium nitrite alone as inhibitor.

For pipe F, the corrosion rate was constant at 0.1605  $\text{g/m}^2\text{hr}$  from 0 to 96 h. It dropped to 0.1204  $\text{g/m}^2\text{hr}$  for the next 48 h and rose again to 0.1605  $\text{g/m}^2\text{hr}$  between 192 and 240 h. It dropped to 0.1204  $\text{g/m}^2\text{hr}$  in the next hour and remained steady through to 288 h. Furthermore, between 0 and 48 h, there was a rise in corrosion rate for pipes E, F, D; it was highest for pipe D, higher for pipe F while pipe E had the least corrosion rate. This implies that at such time, sodium tungstate combined with sodium nitrite had the least corrosion resistance while sodium nitrite combined with zinc nitrite offered better corrosion resistance although, the combined inhibitors with the best performance at such time were those applied to pipe F which is as a result of the improved inhibitive property of both chemicals when mixed relative to other combinations. Again, the use of sodium nitrite and zinc nitrite as inhibitors for corrosion of this type should be discouraged because their combination gave poor performance in terms of pipe protection against microbial corrosion since the calculated corrosion rate was highest (i.e. 0.1204  $\text{g/m}^2\text{hr}$ ) from 48 to 288 h; see Fig. 3.

Fig. 4 shows the results for the three combined inhibitors (sodium tungstate, zinc nitrite and sodium nitrite). From the results, it can be seen that, there was no corrosion for the first 48 h. It rose to 0.0401  $\text{g/m}^2\text{hr}$  in the next one hour and was constant at this rate for the next 48 h. Between 96 and 144 h, no corrosion was recorded but there was an increase in corrosion rate between 144 and 192 h. There was no corrosion between 192 and 240 h. However, the inhibitor performance decreased as the corrosion rate rose from 0 to 0.0401  $\text{g/m}^2\text{hr}$  between 240 and 288 h respectively. Furthermore, comparing the results of Fig. 4 with those of Figs. 2 and 3, it can be seen that the three combinations i.e. sodium tungstate, zinc nitrite and sodium nitrite helped to improve the overall inhibitor performance better than the results obtained for all other inhibitors/formulations (i.e. single and two inhibitor

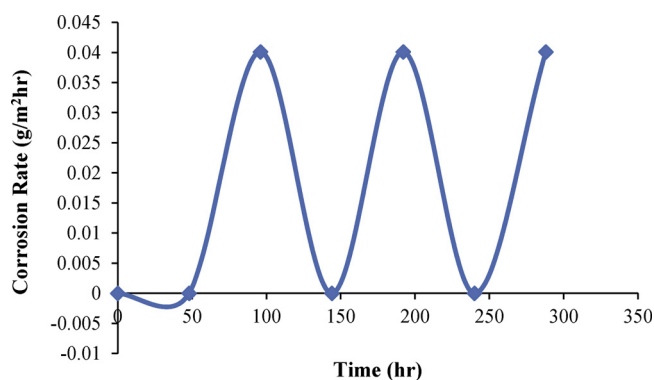


Fig. 4. Corrosion rate of pipe G with time.

combinations) although, when sodium tungstate was used alone as inhibitor, it gave better results relative to other inhibitors hence, the three inhibitors are said to have complemented their individual properties which altered their individual rheological properties for improved resistance against pipe corrosion. In addition, it is believed that between zero and 48 h, the inhibitor formed a passive layer which helped to prevent pipe G from further attack. However, as time elapsed, meso-attack set in which resulted in the removal of the passive/protective layer hence the reason for the increase and fluctuations in corrosion rate between 0 and 288 h as shown in Fig. 4.

Fig. 5 shows the corrosion rates at different times for pipes H, I, and J. For pipe H (pipe without inhibitor in aerobic condition), there was an increase in corrosion rate from 0 to 0.1204  $\text{g/m}^2\text{hr}$  for the first 48 h. It increased to 0.1605  $\text{g/m}^2\text{hr}$  in the next 48 h through to 144 h. The hourly corrosion rate dropped to 0.1204  $\text{g/m}^2\text{hr}$  for the next 48 h and rose back to 0.1605  $\text{g/m}^2\text{hr}$  between 240 and 288 h; see also Table 1, which shows the initial weight, final weight, change in weight and corrosion rate of pipe H from 0 to 288 h.

For pipe I, the corrosion rate was 0.1204  $\text{g/m}^2\text{hr}$  between 1 and 48 h and dropped to 0.0802  $\text{g/m}^2\text{hr}$  for the next 48 h. It rose back to 0.1204  $\text{g/m}^2\text{hr}$  and remained constant through to 144 h. Also, it dropped and remained steady at 0.0802  $\text{g/m}^2\text{hr}$  between 144 and 240 h after which it dropped and remained constant at 0.0401  $\text{g/m}^2\text{hr}$  from 241 h through to 288 h; see also, Table 2 which gives the initial weight, final weight, weight loss and corrosion rate of pipe I between 0 and 288 h.

For pipe J, a constant corrosion rate (i.e. 0.0401  $\text{g/m}^2\text{hr}$ ) was recorded at all times except at the zeroth hour; see Table 3 for the measured weights and corrosion rate of pipe J.

The pipe samples H, I, J were understudied in order to see the effect of not using any inhibitor(s) as a form of pipe protective measure against the use of inhibitors. From the results, it could be seen that the corrosion rate was high and varied between 0.1204 and 0.1605  $\text{g/m}^2\text{hr}$ , 0.1204 and 0.0401  $\text{g/m}^2\text{hr}$  and remained constant (0.0401  $\text{g/m}^2\text{hr}$ ) for pipes H, I and J respectively. Hence, the results of pipes H and I show that oxygen also served as an influence/causative of pipe microbial

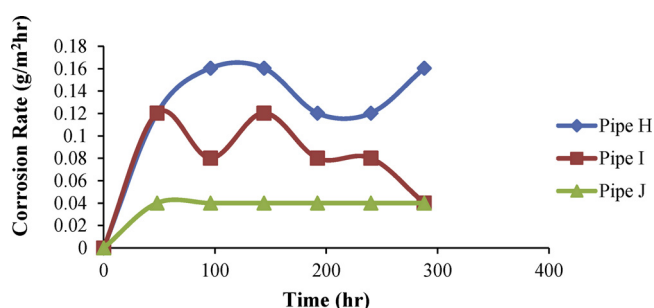


Fig. 5. Corrosion rates of pipes H, I & J with time.

**Table 1**  
Corrosion rate across pipe H.

Time (hr)	W <sub>H1</sub> (g)	W <sub>H2</sub> (g)	W <sub>H2</sub> – W <sub>H1</sub> (g)	C <sub>R</sub> (g/m <sup>2</sup> hr)
0	368.4	368.4	0.0	0.0000
48	368.4	368.1	0.3	0.1204
96	368.1	367.7	0.7	0.1605
144	367.7	367.3	1.1	0.1605
192	367.3	367.0	1.4	0.1204
240	367.0	366.7	1.7	0.1204
288	366.7	366.3	2.1	0.1605

**Table 2**  
Corrosion rate across pipe I.

Time (hr)	W <sub>I1</sub> (g)	W <sub>I2</sub> (g)	W <sub>I2</sub> – W <sub>I1</sub> (g)	C <sub>R</sub> (g/m <sup>2</sup> hr)
0	370.2	370.2	0.0	0.0000
48	370.2	369.9	0.3	0.1204
96	369.9	369.7	0.5	0.0802
144	369.7	369.4	0.8	0.1204
192	369.4	369.2	1.0	0.0802
240	369.2	369.0	1.2	0.0802
288	369.0	368.9	1.3	0.0401

**Table 3**  
Corrosion rate across pipe J.

Time (hr)	W <sub>J1</sub> (g)	W <sub>J2</sub> (g)	W <sub>J2</sub> – W <sub>J1</sub> (g)	C <sub>R</sub> (g/m <sup>2</sup> hr)
0	371.4	371.4	0.0	0.0000
48	371.4	371.3	0.1	0.0401
96	371.3	371.2	0.2	0.0401
144	371.2	371.1	0.3	0.0401
192	371.1	371.0	0.4	0.0401
240	371.0	370.9	0.5	0.0401
288	370.9	370.8	0.6	0.0401

corrosion regardless of whether pipes were submerged or exposed to oxygen since the top surface or bottom layers of soils also contain some amount of oxygen. By comparing the results obtained for pipes H, I and J with those of other inhibitors/formulations used, one could see that the inhibitors actually helped to reduce pipe corrosion except for the pipe protected with sodium nitrite only. Furthermore, the implication is that oxygen corrosion is not as severe as microbial corrosion. Also, combining the three inhibitors improved their overall performance because, it is clear that the inhibitor was able to resist the corrosive effect of oxygen on the pipes, since at some time, the corrosion rate of the pipe dropped to zero for pipe G relative to pipe J (sample for which the corrosion rate was uniform with respect to the exposed sample to oxygen).

### 3.1. Inhibitor efficiencies

In order to estimate the inhibitor efficiencies of Pipes A – G (i.e. pipe samples treated with inhibitors) relative to Pipe H (i.e. pipe without inhibitor in aerobic condition) over a period of 288 h, the average corrosion rates for pipes A–G alongside that of pipe H were all calculated by simply summing up all corrosion rates and dividing through by 6; see Table 4 for the estimated efficiencies of pipes with inhibitor coating as against pipe corrosion measurements under aerobic conditions and without inhibitors. The inhibitor efficiency is given by (2) and  $C_{R0} = 0.1405 \text{ g/m}^2\text{hr}$ .

From the results above, the efficiency of the inhibitor (sodium tungstate only) for pipe A with respect to pipe H (no inhibitor) was 61.90%. This agrees with the findings of Angamuthu et al. [31]; they obtained an efficiency of 65% for the use of sodium tungstate as inhibitor for metallic protection against microbial corrosion. The reason for the slight deviation may be due to environmental factors such as

**Table 4**  
Efficiency of inhibitors relative to aerobic conditions without inhibitor.

Pipes	C <sub>R1</sub> g/m <sup>2</sup> hr	Efficiency (%)
A	0.0535	61.90
B	0.1471	– 4.77
C	0.0936	33.33
D	0.1003	28.56
E	0.0602	57.12
F	0.1404	0
G	0.0201	85.68

temperature. The efficiency of sodium nitrite when used as the only inhibitor (i.e. on pipe B) was found to be -4.77% which implies that the use of sodium nitrite alone as inhibitor against the action of *Acidithiobacillus thiooxidans* for corrosion control should be discouraged as the chemical is highly inefficient when used alone as inhibitor.

The efficiency of inhibitor (zinc nitrite only) for pipe C was 33.33%. This indicates that zinc nitrite alone has little capacity to inhibit this type of corrosion. Again, this is in line with the results of Angamuthu et al. [31] although, an efficiency of 40% was reported in their work.

The efficiency value (28.56%) of the two inhibitors (sodium tungstate and sodium nitrite) for pipe D was also relatively low and suggestive of the fact that, the combined inhibitors can only offer little or no protection for the pipe against the corrosive ability of the microbe.

The efficiency of sodium tungstate and zinc nitrite combined as inhibitors for Pipe E is 57.12% which is also very close to the value (60%) obtained by Angamuthu et al. [31] for the same combination. This result means that the inhibitive power is a little above average, which is quite good. Hence, the combination can be used as a pipe protective measure in combination with other methods such as cathodic protection, lubrication, painting, monitoring and inspection for improved performance.

For pipe F, the efficiency of the inhibitive power of sodium nitrite and zinc nitrite against the corrosive effect of the microbe shows that the two compounds should not be combined as inhibitors as the formulation is highly inefficient in terms of offering resistance to microbial corrosion by the microbe.

The efficiency of the combination of the three inhibitors (sodium tungstate, sodium nitrite and zinc nitrite) for pipe G is highest (i.e. 85.68%). According to Angamuthu et al. [31], an efficiency of 95% was obtained. The results indicate that for maximum protection of the carbon steel pipe against external corrosion, the three inhibitors should be combined for effective microbial corrosion control. The difference between the two results may be as a result of external conditions like exposure to oxygen, type of microbe and other factors.

Also, in order to calculate the inhibitor efficiency for Pipes A–G (with inhibitor) with respect to Pipe I (no inhibitor in anaerobic condition) over a period of 288 h, the average corrosion rate as obtained for Pipe I is 0.0869 g/m<sup>2</sup>hr.

With pipe I (i.e. pipe with no inhibitor in anaerobic condition) as reference, the inhibitor efficiencies of pipes A – G were determined; the results are as shown in Table 5a. The efficiency of the inhibitor (sodium tungstate only) for pipe A is 38.45% which shows that sodium tungstate

**Table 5a**  
Efficiency of inhibitors relative to anaerobic conditions and without inhibitor.

Pipes	C <sub>R0</sub> (Pipe I)	C <sub>R1</sub>	Efficiency (%)
A	0.0869	0.0535	38.45
B	0.0869	0.1471	– 69.28
C	0.0869	0.0936	– 7.71
D	0.0869	0.1003	– 15.42
E	0.0869	0.0602	30.72
F	0.0869	0.1404	– 61.57
G	0.0869	0.0201	76.87

**Table 5b**

Tafel polarization parameters for microbial corrosion of X-52 carbon steel with no inhibitor, in the presence of Sodium tungstate alone, and sodium tungstate + zinc nitrite + sodium nitrite combined @ 30 °C.

Inhibitor	Chemical Vol. (ml)	Ecorr (V/SCE)	-bc (mV/dec)	iCorr (mA/cm <sup>2</sup> )	CR (mmpy)	I.E%
No inhibitor	–	–501	72.27	1.88	456.8	0
ST	10	–362	45.72	2.538	64.97	60
ST + SN + ZN (A <sub>ec</sub> )	30	–482	52.00	0.277	44.55	87.5
ST + SN + ZN (A <sub>naec</sub> )	30	–450	44.33	0.325	52.25	74.6

**Key:**

ST – Sodium Tungstate.

SN – Sodium Nitrite.

ZN – Zinc Nitrite.

(A<sub>ec</sub>) – Aerobic condition.(A<sub>naec</sub>) – Anaerobic condition.

has little inhibitive effect when used alone as inhibitor under anaerobic condition. From the results, it is evidently unadvisable for one to consider the use of any of the inhibitors (sodium nitrite only; zinc nitrite only; sodium tungstate and sodium nitrite; sodium nitrite and zinc nitrite) for pipe microbial corrosion of this kind in anaerobic condition since they all gave low inhibition efficiencies (i.e. efficiencies between -69.28 and 38.45%).

**Table 5b** gives the results obtained from the Tafel polarization measurements. The corrosion inhibition efficiency recorded is 60% for sodium tungstate as the only inhibitor as against, 61.9% estimated from the weight loss measurements which gives an error of 3.1%. Similarly, for the three chemicals combined as inhibitor, the corrosion inhibition efficiency obtained from the polarization studies was 87.5% as against 85.68% for the weight loss measurements; this gives an error/difference of 2.1% thus, the accuracies of the weight loss method lies in the range of 96.9–97.9%.

However, the use of sodium tungstate only and combination of sodium tungstate and zinc nitrite as inhibitors for pipes A and E respectively, gave inhibitor efficiencies of 38.45 and 30.72% which shows the inhibitors are slightly efficient in curbing corrosion of this sort under anaerobic condition. Hence, other corrosion control methods can be adopted in order to boost the corrosion resistance offered by the inhibitors when used to control corrosion of this kind.

Again, the efficiency of the three inhibitors combined (sodium tungstate, sodium nitrite and zinc nitrite) for Pipe G is highest (76.87%) although lower than the value obtained for the aerobic case. This is still indicative of a good inhibitive power i.e. the three inhibitors still retain their inhibitive ability and yet are able to offer significant resistance to microbial corrosion of this nature under anaerobic conditions. Furthermore, comparing this value with the result from Tafel polarization measurements show that, the weight loss method gave a corrosion inhibition efficiency of 2.95% deviation from the Tafel polarization results thus, giving an accuracy of 97.05%.

### 3.2. Optimum inhibitor concentrations

#### 3.2.1. Two inhibitors

(i) For pipe D (sodium tungstate and sodium nitrite); volume of inhibitor used = 10 ml

In **Table 6**, it can be seen that, as the concentration of the inhibitor increased from 0 to 49 g/l between 0 and 120 h, the weight of the pipe kept increasing beyond the initial weight (370.3 g). The weight of the pipe remained constant at 368.6 g between 144 and 168 h after which further increase in inhibitor concentration led to reductions in pipe weight hence, the optimum concentration for the combined inhibitors

**Table 6**

Variation of sodium tungstate and sodium nitrite concentration with pipe weight.

Time (hr)	Inhibitor concentration (g/l)	Weight (g)
0	0	370.3
24	45	370.0
48	46	369.7
72	47	369.4
96	48	369.0
120	49	368.8
144	50	368.6
168	51	368.6
192	52	368.5
216	53	368.3
240	54	368.0
264	55	367.8

was found to be between 50 and 51 g/l.

(ii) Pipe E (sodium tungstate and zinc nitrite); volume of inhibitor used = 10 ml

For sodium tungstate and zinc nitrite combination, the optimum concentration was found to be between 49 and 50 g/l at 120 and 144 h respectively, where there is no weight loss of the pipe as shown in **Table 7**

(iii) Pipe F (sodium nitrite and zinc nitrite); volume of inhibitor used = 10 ml each

As expected, there was no optimum point for both inhibitor combinations and as earlier stated, their combination for use as inhibitor should be discouraged. It is clear that the combined form of both chemicals is passive since continuous weight reduction of the pipe F is evident; **Fig. 6** shows the variation of the weight of pipe F with time for different inhibitor (sodium tungstate and zinc nitrite) concentrations.

#### 3.2.2. Optimum points for 3 combined inhibitors

(i) Pipe G (sodium tungstate, zinc nitrite and sodium nitrite); volume of inhibitor used = 10 ml each

In **Table 8**, the mixed concentration of sodium tungstate, zinc nitrite and sodium nitrite are presented. For the mixed inhibitor concentration of the chemicals, the optimum inhibitor concentration was found to lie between 51 and 52 g/l since the pipe weight was constant at the specified concentrations; the corresponding times are 168 and 192 h respectively. Furthermore, based on the results, it is suggested that further works are conducted in order to understand the chemistry/mechanism behind the improved performance of the three-in-one

**Table 7**

Variation of sodium tungstate and zinc nitrite concentration with pipe weight.

Time (hr)	Inhibitor concentration (g/l)	Weight (g)
0	0	368.5
24	45	368.2
48	46	367.9
72	47	367.6
96	48	367.4
120	49	367.3
144	50	367.3
168	51	367.2
192	52	367.0
216	53	366.7
240	54	366.4
264	55	366.0

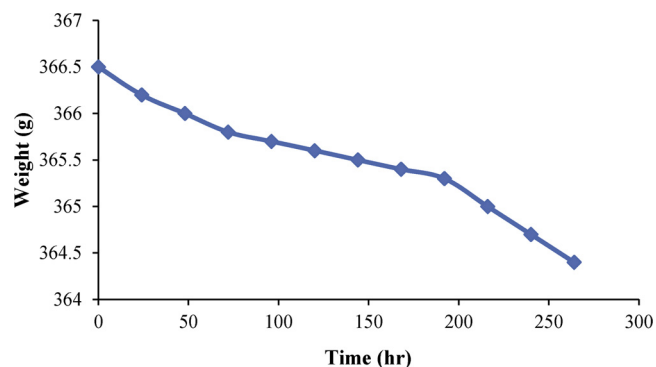


Fig. 6. Variation of pipe weight with time for pipe F.

Table 8

Variation of sodium tungstate, sodium nitrite and zinc nitrite concentration with pipe weight.

Time (hr)	Inhibitor concentration (g/l)	Weight (g)
0	0	370.0
24	45	369.3
48	46	368.8
72	47	368.4
96	48	368.0
120	49	367.8
144	50	367.7
168	51	367.6
192	52	367.6
216	53	367.4
240	54	367.2
264	55	367.0

inhibitor despite the passive behaviour of sodium nitrite in order formulations.

Figs. 7 and 8 show pipes A, H and G before and after corrosion.

### 3.3. Inhibitor-costing

According to the results obtained, the combination of sodium tungstate with zinc nitrite and sodium nitrite as co-inhibitors gave the highest efficiency hence, the inhibitor costs were determined according to their use as contained in Table 9.

Parameters used for costing: pipe length = 0.3 m, diameter = 2 in.

Based on the calculations, it will cost N 4, 250 (naira) worth of inhibitors to protect the surface of a 30 cm long 2-inch diameter carbon steel pipe against microbial corrosion over a period of two weeks, just as it will approximately cost N14, 200 worth of inhibitors to prevent microbial corrosion of a 1 m long, 2-inch diameter carbon steel pipe. Then over a year, the cost of protecting both lengths (0.3 m and 1.0 m) of pipe would be 102,000 naira and 170, 400 naira respectively (Table 9).

### 3.4. SEM and FTIR data for the pipe samples

Since the inhibitor with the three inhibitors combined gave the best performance, further tests (SEM & FTIR studies) were conducted with focus on the three-in-one inhibitor relative to the control samples (i.e. samples without inhibitor in aerobic condition and without inhibitor in anaerobic condition but in the presence of microbes). Fig. 9a and b show the SEM images of the pipe sample G (sample under combined inhibitor protection) with the combined inhibitor spreading over the entire surface of the metal thus creating a protective film which spreads over the surface of the metal i.e., rather than corrosion deposits, oil films in the range of 80–18  $\mu\text{m}$  were spread over the metal surface. The corrosion rate was seen to be lowest for this pipe sample as compared to other pipes protected with other inhibitors (single/combined); also, see Fig. 8 for confirmation of the protective ability of the sodium tungstate + sodium nitrite + zinc nitrite inhibitor. Fig. 10a shows a SEM image of pipe sample H without any form of inhibitor protection but under the combined influence of its exposure to oxygen and microbes; pits and cracks are evident on the surface with an assemblage of damages on the metal surface. The average size of the damage was 20  $\mu\text{m}$  which was seen to have spread over the surface of the metal with a few uniform pits appearing thus confirming the influence of oxygen, while Fig. 10b is the SEM image of pipe J with corrosion products/patches/scales sizing up to 100  $\mu\text{m}$  (i.e. oxygen aided corrosion without microbes). Considering both images in Figs. 10a and b, it could be seen that the corrosive action of *Acidithiobacillus thiooxidans* is more limited under anaerobic conditions relative to its subjection to aerobic condition, hence, the action of the microbe is not favoured by the depletion of oxygen in soils/the environment, which is suggestive of oxygen depletion as a control strategy for the microbial influence of the microbe on pipelines. An optical view of the cultured colony of *Acidithiobacillus thiooxidans* that is not in contact with any pipe is as shown in Fig. 10c; also, the results confirming the biochemical activities of the microbe in different media are reported in Appendix B (Table 12).

Figs. 11 and 12 are plots of absorbance vs wave number for pipe samples J and G respectively, while Figs. 13 and 14 are plots of % transmittance vs wave number for pipe samples A–C and pipe sample H respectively. Based on the FTIR plots in Figs. 11–14, it could be deduced that, from 3000–3700  $\text{cm}^{-1}$ , bonds such as O–H (3640–3610  $\text{cm}^{-1}$ ) stretch, free hydroxyl strong sharp bonds were formed, between 3500–3200  $\text{cm}^{-1}$  O–H stretch, strong, broad, hydrogen bonds were formed which indicate the presence of alkanols and phenols on the metal surface. From 3400–3250  $\text{cm}^{-1}$ , N–H stretch, medium bonds of 1, 2° amines and amides were detected. Between 3300–3270  $\text{cm}^{-1}$ , narrow, strong terminal alkynes were detected and between 3100–3000  $\text{cm}^{-1}$ , strong C–H stretch aromatics and medium C–H stretch double bond alkenes were detected. From 3000–2000  $\text{cm}^{-1}$ , medium C–H stretch bonds of alkanes were detected, from 2830–2695  $\text{cm}^{-1}$ , medium bonds of aldehyde were detected, the following groups below were low in concentrations from the 2500–2000  $\text{cm}^{-1}$  mark i.e. from 2260–2210  $\text{cm}^{-1}$ , C–N triple bonds were detected thus, indicating the presence of nitriles and C–C weak triple bond stretch alkynes. Between 1760 and 1665  $\text{cm}^{-1}$ , strong C–O stretch double bonds were seen

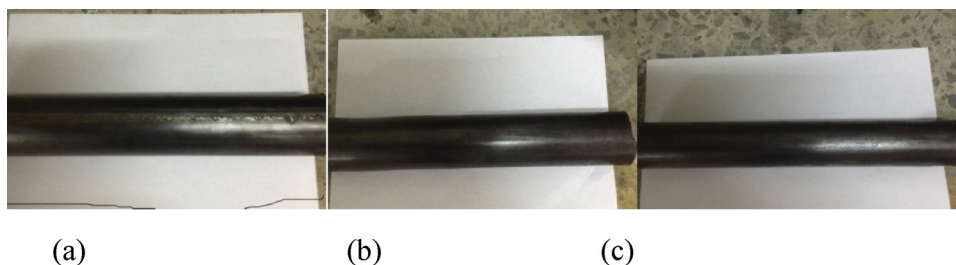


Fig. 7. (a) (b) (c): A view of pipes H, A and G respectively before corrosion.

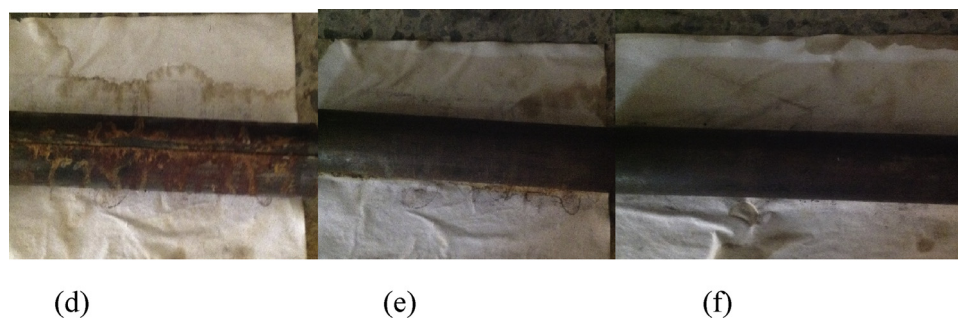


Fig. 8. (d) (e) (f): Pipes H, A and G respectively after corrosion.

Table 9

Cost of the chemicals used in preparing the inhibitors.

Materials	Quantity bought (g)	Quantity used (g)	Total Cost (naira)	Cost of chemicals used (naira)
Sodium tungstate	500	50	27,500	2,750
Sodium nitrite	500	50	6,500	650
Zinc nitrite	500	50	8,500	850
Pipe	10 pieces	1	10,000	Total = 4,200

which indicate the presence of carbonyls thus confirming the adsorption of carboxylic acids from  $1760\text{--}1690\text{ cm}^{-1}$ , esters and saturated aliphatics were seen within  $1750\text{--}1735\text{ cm}^{-1}$ . From  $1740\text{--}1720\text{ cm}^{-1}$ , aldehydes and saturated aliphatics were detected, At  $1730\text{--}1715\text{ cm}^{-1}$ , the presence of  $\alpha$ ,  $\beta$ -unsaturated esters were confirmed. At the  $1715\text{ cm}^{-1}$  mark were ketones and saturated aliphatics while, at  $1710\text{--}1665\text{ cm}^{-1}$ ,  $\alpha$ ,  $\beta$ -unsaturated aldehydes and ketones were seen. Between  $1680\text{--}1640\text{ cm}^{-1}$ , alkenes were identified by C–C stretch medium bonds, At the  $1650\text{--}1580\text{ cm}^{-1}$  region, are N–H normal  $1^\circ$  amine bonds, from  $1600\text{--}1585\text{ cm}^{-1}$  are medium stretch (in-ring) aromatics, at  $1470\text{--}1450\text{ cm}^{-1}$  are medium C–H bend alkanes, at  $1370\text{--}1350\text{ cm}^{-1}$  are medium bonds of C–H rock alkanes, then at  $1360\text{--}1290\text{ cm}^{-1}$  are N–O symmetric bonds of medium stretch nitro compounds, from  $1335\text{--}1250\text{ cm}^{-1}$  are strong C–N stretch aromatic amines, at  $1320\text{--}1000\text{ cm}^{-1}$ , are strong C–O stretch alcohols, carboxylic acids, esters and ethers. Between  $1000\text{--}650\text{ cm}^{-1}$  are strong

bonds of C–H bend alkenes, at  $950\text{--}910\text{ cm}^{-1}$  are medium O–H bend bonds of carboxylic acids, at  $910\text{--}665\text{ cm}^{-1}$  are strong broad N–H wag bonds of  $1^\circ$ ,  $2^\circ$  amines, at  $900\text{--}675\text{ cm}^{-1}$ , are strong C–H “OOP” bonds of aromatics, at  $850\text{--}550\text{ cm}^{-1}$ , are C–Cl medium stretch bonds of alkyl halides, between  $725$  and  $720\text{ cm}^{-1}$ , are medium C–H rock bonds of alkanes, at  $700\text{--}610\text{ cm}^{-1}$  are broad, strong C–H bonds of alkynes while from  $690\text{--}515\text{ cm}^{-1}$ , medium C–Br stretch bonds of alkyl bromides were detected. Again, of all the plots, it could be seen that, pipe G had the highest form of protection across the metal surface except at the  $3700$  or  $400\text{ cm}^{-1}$  mark which may have resulted due to the thin layer of liquid film spread across the metal surface at some points on the metal surface. This implies that the inhibitor was almost evenly distributed over the metal surface/adhered strongly to the metal surface.

However, in Fig. 13, for pipe sample A, the downward peaks/adsorption of groups located at the  $3500\text{ cm}^{-1}$  mark, indicates the presence of O–H stretch hydrogen bonded alcohols and phenols. Another peak is seen at the  $3000\text{--}2850\text{ cm}^{-1}$  mark which confirms the presence of alkanes. From  $1500\text{--}1000\text{ cm}^{-1}$ , other peaks are seen thus confirming the adsorption of aromatics, alkanes, nitro compounds, alkanes, aromatic amines, alcohols, carboxylic acids, esters and ethers. For pipe sample B, the first peak was seen at  $3500\text{ cm}^{-1}$  which also confirms the adsorption of alcohols and phenols. The next peak occurs at  $2000\text{--}1500\text{ cm}^{-1}$  thus confirming the adsorption of alkynes, carbonyls, carboxylic acids, esters, saturated aliphatics, aldehydes, esters, ketones, alkenes,  $1^\circ$  amines, aromatics and nitro compounds; the peaks seen at the  $1000\text{ cm}^{-1}$  mark, confirm the adsorption of alcohols, carboxylic acids, esters and ethers and below  $1000\text{ cm}^{-1}$ , i.e. between  $1000$  and

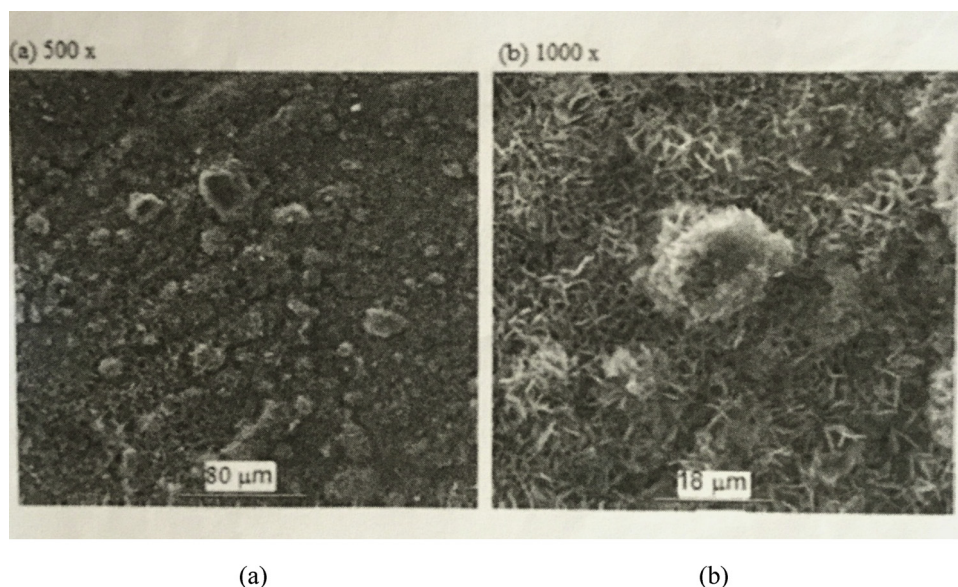
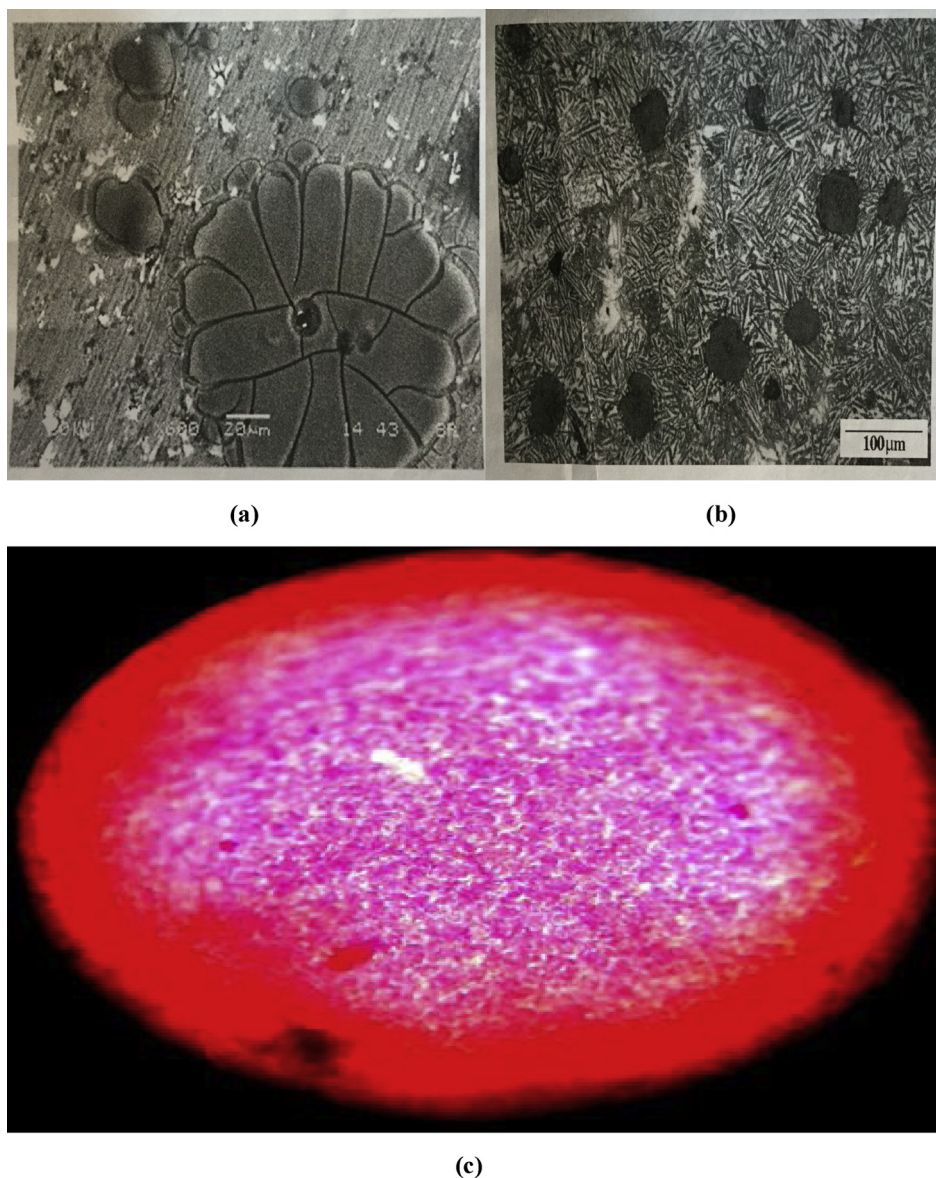
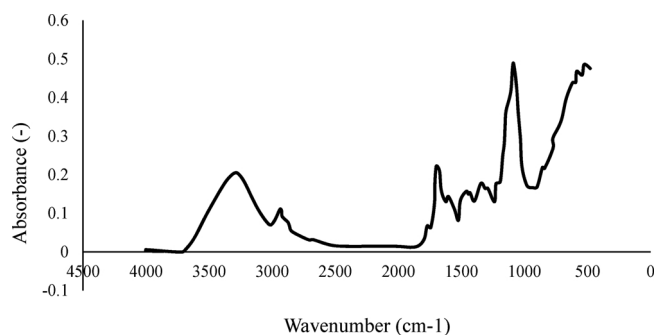


Fig. 9. a. SEM Image of Pipe Sample G b. SEM Image of Pipe Sample G with mag x500 & 1000 oil product/oil film in the range of  $80\text{--}18\text{ }\mu\text{m}$  respectively (best inhibitor performance on pipe).



**Fig. 10.** a. SEM image of the pipe sample H; b. SEM image of pipe sample J (WI, oxygen aided corrosion); c. Screen shot of the rice grain structure of *Acidithiobacillus Thiooxidans* from Ib1290 compound digital LCD inverted biological camera microscope with 5.0 million pixel (MP) infinite optical system.



**Fig. 11.** Absorbance vs wave number of light over the surface of the carbon steel for pipe J (without inhibitor and microbes; oxygen aided corrosion).

650  $\text{cm}^{-1}$ , alkenes were adsorbed and at 690–515  $\text{cm}^{-1}$ , alkyl halides were detected. For pipe C, the first peak is also around the 3500  $\text{cm}^{-1}$  mark thus, confirming the adsorption of phenols and alcohols, the next sharp peak is at 1500  $\text{cm}^{-1}$ , confirming the presence of aromatics, the next peak is at 1000  $\text{cm}^{-1}$ , which confirms the adsorption of alkenes

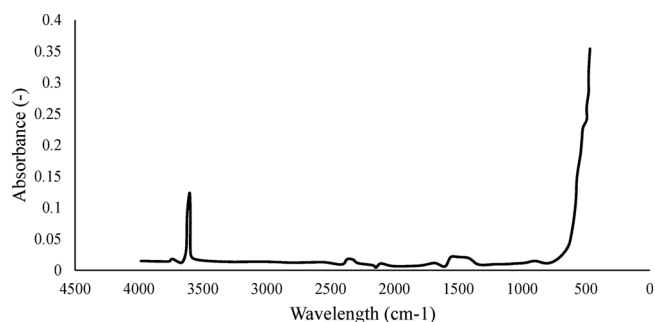


**Fig. 12.** Absorbance vs wave number of light over the surface of the carbon steel For Pipe G (with all three inhibitors).

while the last two peaks lie around 615–515  $\text{cm}^{-1}$ , thus confirming the adsorption of alkyl halides (C-Br stretch bond).

In Fig. 14, the first peak for pipe H lies between 3500 and 3000  $\text{cm}^{-1}$ , which confirms the adsorption of phenols and alcohols. The next is at 3000  $\text{cm}^{-1}$ , which confirms the adsorption of alkenes, at

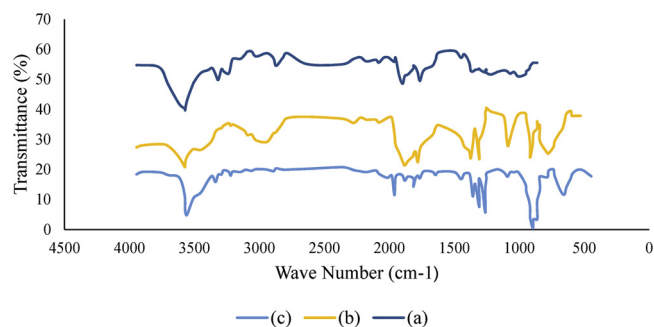


Fig. 13. FTIR Absorbance vs wave number of light over the surface of the carbon steel for Pipes A, B & C; (a) = pipe A, (b) = pipe B and (c) = pipe C.

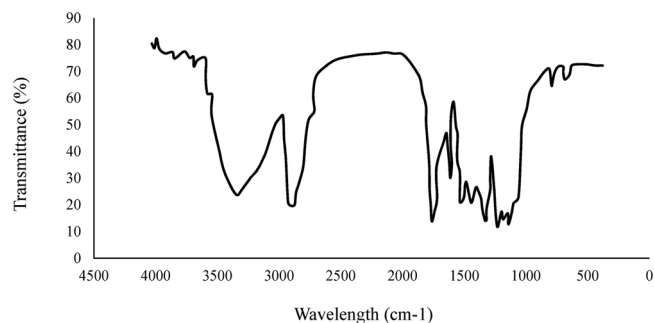


Fig. 14. FTIR Transmittance vs wavenumber for pipe H (without inhibitor under aerobic condition in the presence of microbes).

1760  $\text{cm}^{-1}$ , carbonyls were adsorbed and from 1760–1000  $\text{cm}^{-1}$ , carboxylic acids, esters, aliphatics, aldehydes, saturated aliphatics, esters, ketones, alkenes, 1° amines, aromatics, nitro compounds and aromatic amines were adsorbed, while at 690–515  $\text{cm}^{-1}$ , the presence of alkyl halides was confirmed. Furthermore, it is obvious that, the chemicals used as well as the microbial activities and external sources used to carry out this investigation, such as aerobic and anaerobic environments, brought about some levels of interactions which gave rise to some of the products reported from the FTIR investigation however, it is recommended that further studies be conducted in order to unravel the mechanisms behind these interactions so as to understand the chemistry behind the protections offered and the products formed by reactions that produced the different inhibitors.

### 3.5. Statistical analysis of the weight loss measurements

Results from statistical analysis, such as mean weight loss, confidence interval, variance, standard deviation, coefficient of variation, skew, kurtosis, Kolmogorov Smirnov stat. etc. were examined. Within the 95–99% confidence interval of the analysis, the estimated values lie in the region of 0.10–0.71 for all the pipes. The mean weight of all pipe samples lie in the range of 367.36 (pipe H- lowest)-377.34 g (pipe C- highest). The estimated standard errors were between 0.115 (pipe A- highest) and 0.04 (pipe G- lowest). The estimated variances were in the range of 0.05 (pipe J- lowest)-0.59 (pipe B- highest) with average deviations in the range of 0.09 (pipe G- lowest) - 0.61 (pipe H- highest). The calculated standard deviations are in the range of 0.111 (pipe G- lowest) - 0.77 (pipe B- highest) while the coefficient of variation recorded for all the pipe samples lie within 0.00058 (pipe A- lowest) - 0.00206 (pipes F and J- highest). The skews for the pipe samples were found to be between 0.33 (pipe A- lowest) - 0.66 (pipe B- highest). For the Kurtosis, the estimated values were in the range of -1.517 (pipe A- lowest) to -0.069 (pipe D- highest). The Kolmogorov Smirnov stat. ranged from 0.108 (pipe J- lowest) - 0.1173 (pipe G- highest); the critical K stat values determined at  $\alpha = 0.1, 0.5$  and  $0.01$  respectively were 0.436, 0.483 and 0.576 for each of the pipe samples at those

Table 10

Statistical analysis of weight-loss method for Pipe.A–E.

	Pipe A	Pipe B	Pipe C	Pipe D	Pipe E
Mean	369.13	367.9	377.34	371.54	369.11
Standard error	0.11488	0.29114	0.18754	0.19255	0.12617
95% confidence interval	0.28111	0.71242	0.4589	0.47117	0.30873
99% confidence interval	0.42586	1.0793	0.6952	0.71378	0.4677
Variance	0.092381	0.59333	0.24619	0.25952	0.11143
Average deviation	0.25306	0.6	0.39184	0.39184	0.27347
Standard deviation	0.30394	0.77028	0.49618	0.50943	0.33381
Coefficient of variation	0.00082	0.00209	0.00131	0.00137	0.0009
Skew	-0.33	0.656	0.318	0.551	0.203
Kurtosis	-1.517	-0.218	-0.891	-0.069	-1.46
Kolmogorov-Smirnov stat	0.164	0.127	0.117	0.112	0.168
Critical K-S stat, alpha = .10	0.436	0.436	0.436	0.436	0.436
Critical K-S stat, alpha = .05	0.483	0.483	0.483	0.483	0.483
Critical K-S stat, alpha = .01	0.576	0.576	0.576	0.576	0.576

Table 11

Statistical analysis of weight-loss method for Pipe.F–J.

	Pipe F	Pipe G	Pipe H	Pipe I	Pipe J
Mean	368.2	370.47	367.36	369.47	371.1
Standard error	0.28619	0.042056	0.28607	0.1822	0.08165
95% confidence interval	0.70031	0.10291	0.70002	0.44585	0.1998
99% confidence interval	1.0609	0.1559	1.0605	0.67542	0.30268
Variance	0.57333	0.012381	0.57286	0.23238	0.046667
Average deviation	0.6	0.089796	0.60816	0.39592	0.17143
Standard deviation	0.75719	0.11127	0.75687	0.48206	0.21602
Coefficient of variation	0.00206	0.0003	0.00206	0.0013	0.00058
Skew	0.158	-0.249	0.04	0.345	0
Kurtosis	-1.172	-0.944	-1.201	-1.255	-1.2
Kolmogorov-Smirnov stat	0.13	0.173	0.122	0.142	0.108
Critical K-S stat, alpha = .10	0.436	0.436	0.436	0.436	0.436
Critical K-S stat, alpha = .05	0.483	0.483	0.483	0.483	0.483
Critical K-S stat, alpha = .01	0.576	0.576	0.576	0.576	0.576

conditions, respectively.

The statistical results are shown in Tables 10 and 11. Pipes A and E had the lowest standard error i.e.  $< 0.2$ . This means that corrosion rate with respect to the weight loss was about 80% accurate. Hence, the two samples with sodium tungstate as the only inhibitor and non-microbial aerobic sample respectively were estimated within a good level of accuracy. The validity of the non-microbial aerobic corrosion statistical analysis is dependent on the atmospheric condition. This assertion is validated by the Gumen distribution of sample J and the comparative distribution of samples A and J (Figs. 15a and j). Furthermore, Results of Pipe A were skewed to further buttress on its accuracy. The use of sodium tungstate as the only inhibitor had the highest inhibitor performance going by the Gumen distribution shown in Fig. 15a. Sample G had the least standard deviation and coefficient of variation which is indicative of its best performance and high level of accuracy of the measurements. Sample B has the highest standard deviation and coefficient of variation showing that the sodium nitrite as the only inhibitor is the most inefficient inhibitor. Pipe H gave an average deviation showing the influential role of oxygen on the microbial attack on the carbon steel. More noteworthy is the uniform coefficient of variation in samples F and H. This shows the effects of the nitrites as inhibitors. Sample B has the highest skew thus confirming that sodium nitrite has no significant effect/protection of the carbon steel against microbial degradation. Results of the statistical analyses are as shown in Tables 10 and 11.

Based on the overall result from statistical analyses, a comparative

study was carried out using the Gumen distribution i.e. Figs. 15a–j. Despite the low R-square values displayed for all pipe samples including pipes B, C, D, H and I. The sample in anaerobic condition (sample H) showed the highest correlation with sample A. Samples E, F, G and J showed variances in the levels of protection provided by the inhibitors with respect to samples A and H. Furthermore, these results conform and agree with the experimental outcomes reported in Sections 2.2.1–2.2.5.

Standard error of the mean is a probabilistic statement on how the mean weight of the pipe samples deviate from the average weight loss of each sample; based on the estimated errors i.e. in the range of 0.04 (pipe A)–0.29 (pipes B & H), it implies that the statistical values show a level of accuracy between 96–71%. Comparing the estimated variances, the weight loss determined for the pipe samples are in the range of 0.01 (pipe G)–0.59 (pipe B) which reveals that, the calculated variances per pipe sample are far off the actual mean of the samples by a minimum of 1% and a maximum of 59%. The estimated average deviation reveals how the pipe weights deviate from the average pipe weight per sample; the values range between 0.09 (pipe G)–0.6 (pipes B & F) giving 91–40% closeness. The standard deviation for the samples range between minimum 0.30 (pipe A) - maximum 0.76 (pipes F and H), this is indicative of the way the values/measured weight loss spread from the mean/median weight loss of each pipe sample. The coefficient of variation is the ratio of the standard deviation to the mean; it is a measure of the risks involved in getting the desired results based on the method used. The coefficient of variation for all pipe samples lie in the range of 0.0003 (pipe G)–0.0021 (pipes B & F) which give room to predict accuracies in the range of 99% since the risks are very low i.e. regardless of the low  $R^2$  values indicated in Figs. 15a–j (Appendix A), the higher the risks, the greater the tendencies for inaccuracies in the weight loss measurements. Skewness is a measure of imbalance or asymmetry of a set of data from the mean, however, it measures the degree of distortion to the left or right of a distribution and how it differs from a normal distribution. The estimated skews lie from -0.33 to 0.66 with most of the data skewed to the right, hence the weight loss values recorded do not define a normal distribution but an asymmetric type with the weight loss data positively skewed i.e. the data has a long tail that extends rightwards hence, it is positively skewed with its mean and median weight loss values greater than the modal weight loss. The weight loss data was found to be mesokurtic for pipe J since the estimated Kurtosis was zero for this pipe. Since the estimated Kurtosis are all negative, it implies that the weight loss distribution is characterized by thin tails compared to a normal distribution hence, it is platykurtic. The Kolmogorov values obtained for the weight loss measurements show that the Kolmogorov “Ks” are very close with the lowest value recorded for pipes D and J (i.e. 0.11) and the highest value recorded for pipe G (i.e. 0.17); since the Kol. value is a means of knowing if the estimated weight loss for the pipe samples come from the same data set/belongs to a category i.e. not measured off the distribution, it then implies that all the recorded values are in order and can actually mimic the weight loss of the pipes at the conditions described owing to the lowest percent difference of 35% between the lowest and highest Kolmogorov values; this is further justified by the critical K–S stat. values obtained at  $\alpha = 0.01$  to 0.1 which give same values per fixed value (see Tables 10 and 11).

### 3.6. Tafel polarization measurements for corrosion of the X-52 carbon steel

Concerning the corrosion rate of X-52 carbon steel in the absence of any inhibitor, the corrosion rate was high. The application of inhibitor to the metal surface actually helped to bring down the corrosion current alongside the corrosion rate to a bearable rate. Inhibition efficiency was found to increase with increased concentrations of the three chemicals combined as inhibitor but this effect was more significant when the microbes in contact with the lubricated carbon steel were exposed to oxygen than when they were devoid of oxygen. The efficiency of the

three combined chemicals (ST, SN and ZN) in anaerobic and aerobic conditions were higher than the case of ST only in contact with the metal exposed to the microbes giving an optimum inhibitor concentration of 51–52 g/L with equal portions of ST, ZN and SN. Also, considering Table 5b, there is a positive shift in the  $E_{\text{corr}}$  value and according to Li et al. [32], when the shift in potential exceeds  $\pm 85\text{mV}$  with respect to the case of the no inhibitor carbon steel, the inhibitor then behaves as either an anodic or cathodic type inhibitor whereas, in the current study, the maximum displacement in the  $E_{\text{corr}}$  was found to be in the region of + 15 mV which is an indication that the three chemicals act as mixed type inhibitor which may be accompanied by hydrogen evolution and dissolution of the carbon steel [33]. From the values obtained i.e. Table 5b, the polarization values, corrosion of the metal may be evident due to anodic oxidation of the steel caused by dissolution of the metal. The values also give a clear indication that, the cathode may exhibit a non-linear behaviour since the values of the cathodic slope vary significantly with increased inhibitor concentration until the optimum point thus exhibiting a non-linear behavior and this is indicative of hydrogen evolution as non-activation-controlled, i.e. the presence of inhibitor alters the inhibition mechanism of sodium tungstate in the mixed phase.

### 3.7. Some insights on the reasons for the low performances of the sodium and zinc nitrite-inhibitors

Sodium nitrite, an anodic inhibitor and zinc oxide, a cathodic inhibitor, have been reported to be able to combat corrosion induced by chlorinated water/chlorides on steel embedded in concrete containing quarry dust of crushed blue stone as fine aggregates for construction purposes. This investigation was carried out to understudy the use of quarry sand as replacement for sand in the construction industry. 1–4% ZnO and 1–4%  $\text{NaNO}_2$  were used as corrosion inhibitors for steel structures. It was recorded that at an optimum concentration of 2%,  $\text{NaNO}_2$  and ZnO absorbed more water and began to lose their inhibition characteristics thus, there was high corrosion rate in the concrete structures. In addition, the inorganic inhibitors could no longer prevent the chloride ions from reacting with the ferrous ions hence, there was zero or low anodic shift in the corrosion potential which forced the metallic surface to remain in active state [34]. Beyond the optimum concentration, an increase in percentage of inhibitors increased the corrosion rates. Methods adopted in this study include: impressed voltage method, rapid chloride ion penetration test, AC impedance measurement and weight loss measurement. Beyond 2%, the tensile and flexural strengths of the steel reduced significantly giving an optimum concentration of 2% as the best inhibitor. This further implies that, despite their inhibitory potentials, the concentration /percentages of these inhibitors or those of their composites must be monitored when applied to corrosion prone surfaces. The corrosion initiation time was also seen to be earlier for  $\text{NaNO}_2$  than for ZnO which confirms the loss of protective abilities of the inhibitors. The  $\text{NaNO}_2$  protected steel was seen to have lost more weight than that of ZnO [35]. Borrowing a leaf from this study, it then implies that when a compound of zinc such as  $\text{ZnNO}_2$  is used in mixed form with sodium nitrite, the tendency to reduce their performances may be enhanced. In an investigation to compare sodium nitrite, trisodium citrate (TSC) and TSC–zinc acetate as corrosion inhibitors for steel rebar in simulated concrete interstitial solution containing chloride, at low concentrations,  $\text{NaNO}_2$  acted as a corrosion stimulant, while at increased concentration, the  $\text{NaNO}_2$  protection efficiency was enhanced. Overall, trisodium citrate offered better protection than  $\text{NaNO}_2$  but in the presence of TSC–zinc acetate, the corrosion rate dropped significantly and based on Tafel polarization studies, concrete pore solution contaminated with 3.5% NaCl can be well protected with TSC 100 ppm–ZnAc 50 ppm concentrations [36]; in their work, FT-IR and UV–vis spectral studies and optical microscopic investigations revealed the mechanism of interaction of compounds on steel rebar. Inhibitors are known to influence the chemistry/kinetics of

electrochemical processes [34,37,38]. For metals in contact with chlorinated water as corrosion stimulant, the mechanisms by which corrosion inhibitors prevent corrosion of metals include (i) low rate of diffusion of the corrosion stimulating agent i.e. chloride ion (ii) A rise in the quantity of bound chloride (iii) increase in the corrosion-stimulant's threshold concentration i.e. chloride ion threshold value (iv) inhibition of the anodic, cathodic or both reactions [39–42]. Based on the failure of some known inhibitors recorded in some works, the authors argued that some of the claims as regards the inhibitors were not similar [43], whereas, for other authors, some of the compounds were found to be effective in lowering the corrosion rate of steel rebar in concrete [44,45]. Supernatant solutions of *Acidithiobacillus thiooxidans* (*At. thiooxidans*), *Acidithiobacillus ferrooxidans* (*At. ferrooxidans*), and *Aspergillus Niger* (*A. Niger*) were used to absorb and dissolve metals contained in slags obtained during steel casting process. *At. thiooxidans* supernatant culture of 0.016 M H<sub>2</sub>SO<sub>4</sub> was the most effective bio-leaching agent for metals extracted from slag via Electric Arc Furnace method (EAF). Maximum extraction for Mg was 28%, while it was 0.1% for molybdenum after six days. Repeated bioleaching cycles increased metal recovery from 28 to 75%, 14–60% and 11–27%, for Mg, Zn and Cu respectively. This reveals that *At. Thiooxidans* has high affinity for zinc metal based on their investigation hence, it must have reduced the proportion of the metallic constituents/components in the inhibitor. Although, this study did not report on the extraction of Na, however, the percentage removal range of Zn i.e. 14–60%, from its compound reveals the potential of this microbe for Na extraction since the reported metals are alkali metals of which Na is no exception [46]. An investigation carried out by Liu et al. [47], revealed that *Acidithiobacillus thiooxidans* has the ability to remove cadmium from soils which also confirms the microbe's affinity for metals, hence, they proposed the need to carry out further investigations in order to understudy the affinity of *At. thiooxidans* for Na metal in its compounds; this will also unveil its reduction mechanism of metals in compounds or its interactions with these metals.

#### 4. Conclusion

Microbial corrosion of the external surface of a carbon steel pipe caused by the action of *Acidithiobacillus thiooxidans* can best be controlled using sodium tungstate, sodium nitrite and zinc nitrite combined as inhibitor rather than using each inhibitor alone or combining any two of the three inhibitors. Zinc nitrite and sodium nitrite combination should not be considered as inhibitor combinations because, combinations of this kind are not resistant to microbial corrosion of this sort. However, for optimum inhibitor performance with minimal cost implications, the optimum concentration of the three combined inhibitors was found to lie between 51 and 52 g/l. The inhibitor performance was poorer under anaerobic conditions, which implies that if higher inhibitor efficiency is desired, the use of the formulation in aerobic conditions is necessary considering the fact that oxygen enhances the microbial activity of the microbe. The cost of maintaining a carbon steel pipe with the three chemical combination in the referred microbe's environment is quite economical. Also, based on the statistical analyses, the statistical results for sample A conform to the results of the experiments. There exists a strong correlation between the results obtained for samples A and H which suggests that, depleting the amount of oxygen in soils where these pipelines are placed is as effective as applying sodium tungstate only as corrosion inhibitor to the surface of pipes in contact with the microbes in aerobic condition. Based on the performance of the three chemicals (sodium tungstate + sodium nitrite + zinc nitrite), the performance increased by 38% (i.e. 85.68%) as against the performance of 61.9% recorded for sodium tungstate only, as inhibitor for X-52 carbon steel. Based on findings, the low and poor performances of sodium and zinc nitrites respectively, may be as a result of the reduction reactions of *At. Thiooxidans* on both compounds, since there is ample evidence that the bacteria has high affinity for zinc

and alkali metals. Also, the interactions of the mixed inhibitors may have resulted in the formation of substances that accelerated the corrosion rate, since *At. thiooxidans* thrives more in acidic medium. At low concentrations, NaNO<sub>2</sub> may act as a corrosion stimulant, hence, there is need to optimize the solution concentration of this inhibitor when used.

#### Conflict of interest disclosure

The authors hereby declare that there is no conflict of interest regarding the publication of this paper.

#### Funding

This research did not receive any specific grants of funding from any institution or any public commercial or non-profit agency.

#### Data availability

The data provided in this study are enough to guarantee any form of reproducibility required for this/further research.

#### Acknowledgement

The authors wish to thank Covenant University for providing the required sponsorship at different stages of this research. The authors also appreciate Sanni Samuel for conceptualizing the subject, planning out the experimental study and preparing the manuscript, Ewetade Peters for carrying out the experimental work, Emetera Moses for the statistical data generation, Oluranti Agboola and Emeka Okoro for their corrections and useful hints that added much value to the work as well as Mr Shade Olorunshola and Mr Taiwo Olugbenga for culturing the microbe and carrying out the necessary tests to ascertain the presence and growth of the microbe in the culture-medium.

#### Appendix A. Supplementary data

Supplementary material related to this article can be found, in the online version, at doi:<https://doi.org/10.1016/j.mtcomm.2018.12.010>.

#### References

- [1] S.S. Al-Jaroudi, A. Ul-Hamid, M.M. Al-Gahtani, Failure of crude oil pipeline due to microbiologically induced corrosion, *Institute of Materials, Miner. Min.* 46 (4) (2011) 568–579.
- [2] R. Aruliah, M. Sundaram, P. Narayanan, R. Annamalai, Biodegradation of corrosion inhibitors and their influence on petroleum product pipeline, *Microbiol. Res.* 162 (2007) 355–368.
- [3] E. Cantero-Valencia, J.J. Peña-Cabriales, Effects of iron-reducing bacteria on carbon steel corrosion induced by thermophilic sulfate-reducing consortia, *J. Microbiol. Biotechnol.* 24 (2014) 280–286.
- [4] U.S. Carsten, et al., Impact of nitrate on the structure and function of bacterial biofilm communities in pipelines used for injection of seawater into oil fields, *Appl. Environ. Microbiol.* 74 (9) (2008) 2841–2851.
- [5] E. Dennis, G. Julia, Corrosion of iron by sulfate-reducing bacteria: new views of an old problem, *Appl. Environ. Microbiol.* 80 (4) (2014) 1226–1236.
- [6] A.V. Héctor, K.H. Liz, Microbiologically influenced corrosion: looking to the future, *Int. Microbiol.* 8 (2005) 169–180.
- [7] Hendrik, et al., Accelerated cathodic reaction in microbial corrosion of iron due to direct electron uptake by sulfate-reducing bacteria, *Corros. Sci.* 66 (2013) 88–96.
- [8] C. Hubert, M. Nemati, G. Jenneman, G. Voordouw, Corrosion risks associated with microbial souring control using nitrate or nitrite, *Appl. Microbiol. Biotechnol.* 68 (2005) 212–282.
- [9] P.W. Iverson, I.Laskin Allen (Ed.), *Advances in Applied Microbiology*, vol. 32, Academic Press Inc. Ltd., London, UK, 1987.
- [10] J. Lin, R. Ballim, Review- biocorrosion control: current strategies and promising alternatives, *Afr. J. Biotechnol.* 11 (91) (2012) 15736–15747.
- [11] T. Wu, M. Yan, D. Zeng, J. Xu, C. Sun, C. Yu, W. Ke, Hydrogen permeation of X80 steel with superficial stress in the presence of sulfate-reducing bacteria, *Corros. Sci.* 91 (2005) 86–94.
- [12] T. Wu, M. Yan, J. Xu, Y. Liu, C. Sun, W. Ke, Mechano-chemical effect of pipeline steel in microbiological corrosion, *Corros. Sci.* 108 (2016) 160–168, <https://doi.org/10.1016/j.corsci.2016.03.011>.
- [13] F. Batmangeli, L. Li, Y. Seo, Influence of multispecies biofilms of *Pseudomonas*

- aeruginosa* and *Desulfovibrio vulgaris* on the corrosion of cast iron, *Corros. Sci.* 121 (2017) 91–104, <https://doi.org/10.1016/j.corsci.2017.03.008>.
- [14] R. Jia, D. Yang, D. Xu, T. Gu, Electron transfer mediators accelerated the micro-biologically influenced corrosion against carbon steel by nitrate reducing *Pseudomonas aeruginosa* biofilm, *Bioelectrochemistry* 118 (2017) 38–46, <https://doi.org/10.1016/j.bioelechem.2017.06.013>.
- [15] H. Liu, T. Gu, M. Asif, G. Zhang, H. Liu, The corrosion behaviour and mechanism of carbon steel induced by extracellular polymeric substances of iron-oxidizing bacteria, *Corros. Sci.* 114 (2017) 102–111, <https://doi.org/10.1016/j.corsci.2016.10.025>.
- [16] N. Muthukumar, A. Rajasekar, S. Ponmariappan, S. Mohanan, S. Maruthamuthu, S. Muralidharan, P. Subramanian, N. Palaniswamy, M. Raghavan, Microbiologically influenced corrosion in petroleum products pipelines- a review, *Indian J. Exp. Biol.* 41 (2003) 1012–1022.
- [17] N.C. Ngobiri, E.E. Oguzie, N.C. Oforika, O. Akaranta, Comparative study on the inhibitive effect of Sulfadoxine–Pyrimethamine and an industrial inhibitor on the corrosion of pipeline steel in petroleum pipeline water, *Arab. J. Chem.* (2015) 1–11 received 10 February 2014; accepted 8 April, Article in Press.
- [18] R. Jia, J.L. Tan, P. Jin, D.J. Blackwood, D. Xu, T. Gu, Effect of biogenic H<sub>2</sub>S on microbiologically influenced corrosion of C1018 carbon steel by sulfate reducing *Desulfovibrio vulgaris* biofilm, *Corros. Sci.* 130 (2018) 1–11, <https://doi.org/10.1016/j.corsci.2017.10.023>.
- [19] W. Dec, M. Mosialek, R.P. Socha, M. Jaworska-Kik, W. Simka, J. Michalska, Effect of sulfat-reducing bacteria biofilm on passivity and development of pitting on 2205 duplex stainless steel, *Electrochim. Acta* 212 (2016) 225–236, <https://doi.org/10.1016/j.electacta.2016.07.043>.
- [20] E. Zhou, H. Li, C. Yang, J. Wang, D. Xu, D. Zhang, T. Gu, Accelerated corrosion of 2304 duplex stainless steel by marine *Pseudomonas aeruginosa* biofilm, *Int. J. Biodeterior. Biodegrad.* 127 (2018) 1–9, <https://doi.org/10.1016/j.ibiod.2017.11.003>.
- [21] E. Li, J. Wu, D. Zhang, Y. Sun, J. Chen, D-phenylalanine inhibits the corrosion of Q235 carbon steel caused by *Desulfovibrio* Sp, *Int. Biodeterior. Biodegrad.* 127 (2018) 178–184, <https://doi.org/10.1016/j.ibiod.2017.11.027>.
- [22] L.T. Popoola, S.A. Grema, G.K. Latinwo, B. Gutti, A.S. Balogun, Corrosion problems during oil and gas production and its mitigation, *Int. J. Ind. Chem.* 4 (2013) 35.
- [23] C.A.H. Vonwolzen, Unity of aerobic and anaerobic iron corrosion process in the Soil, *Corrosion* 17 (1961) 119–125.
- [24] L. Erik, S. Wolf-Dieter, L. Eberhard, U.W. Hans, tungsten, tungsten alloys, and tungsten compounds, *Ullmann's Encyclopedia of Industrial Chemistry*, Wiley-VCH, Weinheim, 2000, [https://doi.org/10.1002/14356007.a27\\_229](https://doi.org/10.1002/14356007.a27_229).
- [25] Y. Xue, G. Voordouw, Control of microbial sulfide production with biocides and nitrates in oil simulating reservoir bioreactors, *Front. Microbiol.* 6 (2015) 1–11.
- [26] F. Caleyo, J.C. Velázquez, A. Valor, J.M. Hallen, Probability distribution of pitting corrosion depth and rate in underground pipelines: a Monte Carlo study, *Corrosion Sci.* 51 (2009) 1925–1934.
- [27] J.C. Velázquez, J.A.M. Van Der Weide, E. Hernández, H.H. Hernández, Statistical modelling of pitting corrosion: extrapolation of the maximum pit depth-growth, *Int. J. Electrochem. Sci.* 9 (2014) 4129–4143.
- [28] H. Finner, P. Kernb, M. Scheer, On some compound distributions with Borel summands, *Insurance: Math. Econ.* 62 (2015) 234–244.
- [29] P.P. Kumari, P. Shetty, S.A. Rao, Electrochemical measurements for the corrosion inhibition of mild steel in 1 M hydrochloric acid by using an aromatic hydrazide derivative, *Arab. J. Chem.* 10 (2017) 653–663.
- [30] S. Shahin, S. Bilgic, H. Yilmaz, The inhibition effects of some cyclic nitrogen compounds on the corrosion of steel in NaCl, *Appl. Surf. Sci.* 195 (2003) 1–7.
- [31] A. Angamuthu, C. Thangavelu, S. Rajendran, T. Asokan, Sodium tungstate – Zn<sup>2+</sup> as corrosion inhibitor for carbon steel, *ZAŠTITA MATERIJALA* 53 (2012) 1–6.
- [32] W.H. Li, Q. He, C.L. Pei, B.R. Hou, Experimental and theoretical investigation of the adsorption behaviour of new triazole derivatives as inhibitors for mild steel corrosion in acid media, *Electrochim. Acta* 52 (2007) 6386–6397.
- [33] W. Li, Q. He, S. Zhang, C. Pei, B. Hou, Some new triazole derivatives as inhibitors for mild steel corrosion in acidic medium, *J. Appl. Electrochem.* 38 (2008) 289–295.
- [34] S. Joiret, M. Keddam, X.R. Nóvoa, M.C. Pérezb, C. Rangelc, H. Takenouti, Use of EIS, ring-disk electrode, EQCM and raman spectroscopy to study the film of oxides formed on steel in 1 M NaOH, *Cement Concrete Compos.* 24 (2002) 7–15.
- [35] M. Devi, K. Kannan, Evaluation of corrosion inhibition performance of zinc oxide and sodium nitrite in Quarry dust concrete, *Asian J. Chem.* 25 (15) (2013) 8690–8696, <https://doi.org/10.14233/ajchem.2013.15237>.
- [36] B.P. Maliekkal, J.T. Kakkassery, V.R. Palayoor, Efficacies of sodium nitrite and sodium citrate–zinc acetate mixture to inhibit steel rebar corrosion in simulated concrete interstitial solution contaminated with NaCl, *Int. J. Ind. Chem.* 9 (2018) 105–114, <https://doi.org/10.1007/s40090-018-0142-7>.
- [37] H. Oranowska, Z. Szklarska-Smialowska, An electrochemical and ellipsometric investigation of surface films grown on steel in saturated calcium hydroxide solutions with or without chloride ions, *Corros. Sci.* 21 (1981) 735–747.
- [38] C. Andrade, M. Keddam, X.R. Nóvoa, M.C. Pérez, C.M. Rangel, H. Takenouti, Electrochemical behaviour of steel rebars in concrete: influence of environmental factors and cement chemistry, *Electrochim. Acta* 46 (2001) 3905–3912.
- [39] C.J. Kitowski, H.G. Wheat, Effect of chlorides on reinforcing steel exposed to simulated concrete solutions, *Corrosion* 53 (1997) 216–226.
- [40] K.Y. Ann, H.W. Song, Chloride threshold level for corrosion of steel in concrete, *Corros. Sci.* 49 (2007) 4113–4133.
- [41] S. Trépanier, B. Hope, C. Hansson, Corrosion inhibitors in concrete, *Cement Concrete Res.* 31 (2001) 713–718.
- [42] L. Jiang, G. Huang, J. Xu, Y. Zhu, L. Mo, Influence of chloride salt type on threshold level of reinforcement corrosion in simulated concrete pore solutions, *Constr. Build. Mater.* 30 (2012) 516–521.
- [43] B. Elsener, M. Büchler, F. Stalder, H. Böhm, Migrating corrosion inhibitor blend for reinforced concrete: part 2—inhibitor as repair strategy, *Corrosion* 56 (2000) 727–732.
- [44] W. Morris, M.A. Vázquez, Migrating corrosion inhibitor evaluated in concrete containing various contents of admixed chlorides, *Cement Concrete Res.* 32 (2002) 259–267.
- [45] A. Rosenberg, Discussion: migrating corrosion inhibitor blend for reinforcing concrete: part 1—prevention of corrosion, *Corrosion* 56 (2000) (2000) 986–987.
- [46] H. Hocheng, C. Su, U.U. Jadhav, Bioleaching of metals from steel slag by *Acidithiobacillus thiooxidans* culture supernatant, *Chemosphere* 117 (2014) 652–657, <https://doi.org/10.1016/j.chemosphere.2014.09.0>.
- [47] H.H. Liu, C.-W. Chiu, Y.-C. Cheng, The Effects of Metabolites from the Indigenous *Acidithiobacillus Thiooxidans* and temperature on the bioleaching of cadmium from Soil, Wiley Periodicals Inc, Wiley InterScience, 2003, <https://doi.org/10.1002/bit.10714> www.interscience.wiley.com).